DESIGN OF GENERAL LATTICE STRUCTURES FOR LIGHTWEIGHT AND COMPLIANCE APPLICATIONS

Dr. David Rosen, Dr. Scott Johnston, Marques Reed
The George W. Woodruff School of Mechanical Engineering
Georgia Institute of Technology
Atlanta, GA 30332-0405

Dr. Hongqing Wang
IronCAD Corporation
Atlanta, GA

ABSTRACT
The primary goal is to design parts with lattice mesostructure and demonstrate that they have better structural and/or compliance performance, per weight, than parts with bulk material, foams, or other mesostructured approaches. Mesostructure refers to features within a part that have sizes between micro and macro-scales, for example, small truss structures, honeycombs, and foams. The versatility of additive manufacturing allows for the fabrication of these complex unit cell lattice structures which can be used as building blocks for macro-scale geometries. A method and software system have been developed to synthesize lattice mesostructure parts and compliant mechanisms in 2D and 3D. Underlying the synthesis method is a new analytical model of unit lattices, used to compose larger structures. Axial, bending, shearing, and torsion effects are included in the analysis for each strut in the lattice structure which is then related to the mesostructure level (unit cell). A unit lattice finite element analysis method allowing non-linear deformation is employed to analyze a unit cell comprised of n^3 unit structures for their stiffness and displacement compared to their relative density under loading. Aerospace and biomedical applications are demonstrated.

1 INTRODUCTION TO MESOSTRUCTURED MATERIALS

"When modern man builds large load-bearing structures, he uses dense solids; steel, concrete, glass. When nature does the same, she generally uses cellular materials; wood, bone, coral. There must be a reason for it" (Ashby *et al*., 2000). The key advantage offered by cellular materials is high strength accompanied by a relatively low mass. These materials can provide good energy absorption characteristics and good thermal and acoustic insulation properties as well (Gibson & Ashby, 1997). Cellular materials include foams, honeycombs, lattices, and similar constructions. When the characteristic lengths of the cells are in the range of 0.1 to 10 mm, we refer to these materials as mesostructured materials.

Cellular materials are classified by the nature of the internal voids – either stochastic or ordered. Stochastic materials, such as foams, have excellent thermal and acoustic insulation properties (Ashby *et al*., 2000). Ordered cellular materials, such as honeycombs and lattices, have superior mechanical properties, including energy absorption, strength, and stiffness (Gibson & Ashby, 1997), as well as lower pressure drop and high surface area densities, which are important for heat transfer performance. The largest limitation of stochastic cellular structures is the lack of freedom given to the designer with regards to the topology of the mesostructure (Evans et al., 2001). As such, the focus in this work is on designed lattice structures.

In the past 10 years, the area of lattice materials has received considerable attention due to their inherent advantages over foams in providing light, stiff, and strong materials (Ashby *et al*., 2000). Lattice structures tend to have geometry variations in three dimensions; some of our designs are shown in Figure 1. As Deshpande, Fleck, and Ashby (2001) point out, the strength of foams scales as $\rho^{1.5}$, whereas lattice structure strength scales as ρ, where ρ is the volumetric density of the material. As a result, lattices with a $\rho = 0.1$ are about 3 times stronger than a typical foam. The strength differences lie in the nature of material deformation: the foam is governed by cell wall bending, while lattice elements stretch and compress. The examples in Fig. 1 utilize the octet-truss (shown on the left), but many other lattice structures have been developed and studied (e.g., kagome, Kelvin foam). We have developed methods for designing lattice mesostructure for parts (Wang & Rosen, 2003) and have developed design-for-manufacturing rules for their fabrication in Stereolithography (SL).

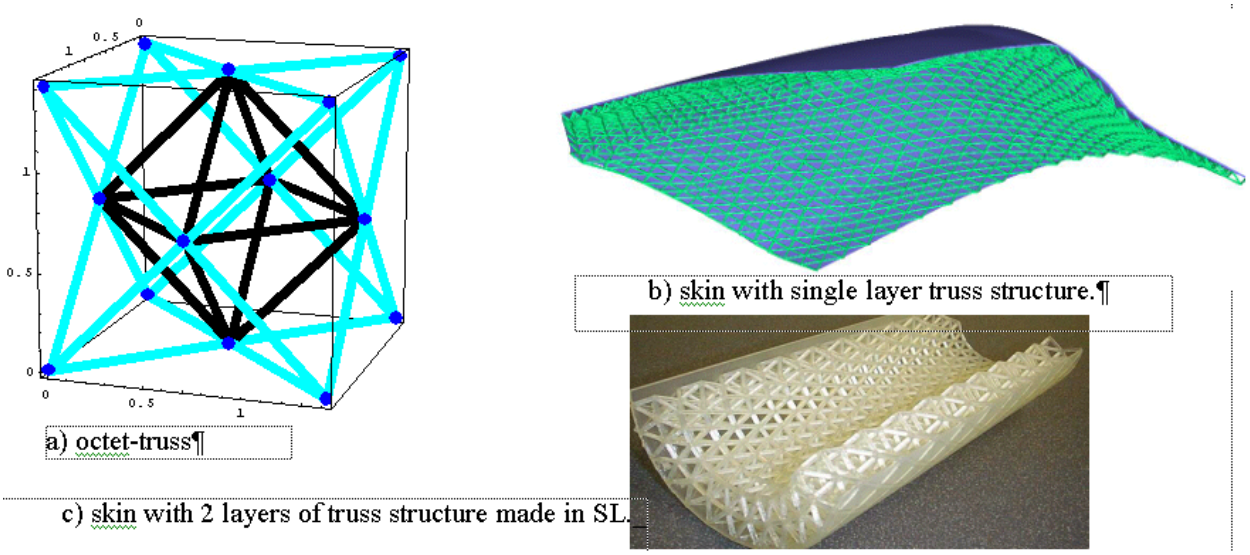

Figure 1. Octet-truss unit cell and example parts with octet-truss mesostructures.

The concept of mesostructured materials is motivated by the desire to put material only where it is needed for a specific application. The area of compliant mechanisms shares the same motivation, where the local compliance of the structure enables the mechanism to perform specified motions. Figure 2 shows an example of a compliant mechanism that acts as a "pore opening" device: the internal pores open when the structure is compressed. A unit cell is shown enlarged on the left. Structures like this may be used in some filtering applications where the

filtering medium is subjected to compressive forces that aid liquid-solid separation. We have built this using SL with pore sizes down to 12x2 mm.

Considerable work has addressed the analysis of mesostructured materials and parts that comprise these materials. Some research addresses the manufacture of parts with mesostructure. Research in shape and topology optimization has dealt with some mesostructure issues, particularly homogenization-based methods. In the area of compliant mechanisms, very good methods have been developed to design 2D mechanisms. Some of these methods apply to the more general problem of designing parts with mesostructure.

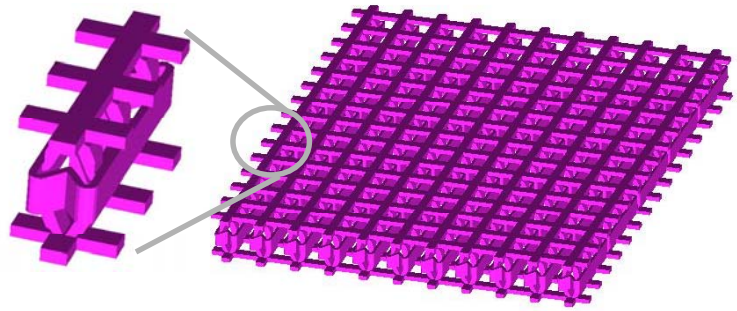

Figure 2. Compliant mechanism: pore opening structure.

We hypothesize that designed mesostructures will enable structures and mechanisms to be designed that perform better than parts with bulk or non-designed mesostructures. To demonstrate progress, we present a structural analysis method for lattice structures, compare it to previous models, show how it can be applied to synthesize structures and mechanisms, and present an example. If successful, this research could provide a significant benefit to society by providing products that utilize material much more efficiently than currently possible, leading to improved fuel economy for cars and planes, robot arms with better performance (lighter weight), prosthetics that adapt to their wearers, and improved filtration media (designed compliance can aid solid-liquid separation), among other benefits. Other broader impacts will be achieved.

2 STRUCTURAL ANALYSIS OF LATTICE MATERIALS

Methods of continuum mechanics have been applied to various mesostructured materials. Ashby and co-workers wrote a book on metal foam design and analysis (Ashby et al., 2000). They and others have applied similar methods to the analysis of lattice structures. The octet truss in Fig. 1 has been extensively analyzed. Deshpande et al. (2001) treated the octet truss unit cell as a collection of tension-compression bars that are pin-jointed at vertices and derived analytical models of their collapse behavior for many combinations of stresses. Wang and McDowell (2005) extended this study to include several other lattice cells.

Recently, we have developed a more general analytical model of lattice behavior. From our general model, models for octet and other truss structures can be derived. We base our model on a single vertex with a collection of struts incident on that vertex, as shown in Figure 4. This vertex model will be our base "unit cell" for representation and modeling purposes.

Lattice unit cells (unit lattices) are parameterizable, analyzable, patternable and manufacturable to support the design. In R^2, each end point of a connected strut has 3 degrees of freedom (DOFs): horizontal displacement, vertical displacement, and in-plane rotation. In R^3, each has 6

DOFs including 3 displacements and 3 rotations. Figure 4 shows a 2D unit lattice, which has $3\times(N+1)$ DOFs. $\underset{\sim}{f}^{(i)}$ are the external forces acting on the node and the end points of the i^{th} strut in R^3. The design variables of the unit lattice in a given topology are strut geometry, such as diameter for uniform cylindrical struts, two end diameters for conic struts, or length and width for uniform rectangular struts.

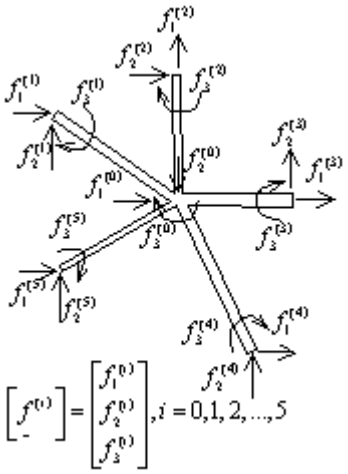

Figure 3. A Typical Unit Truss Model

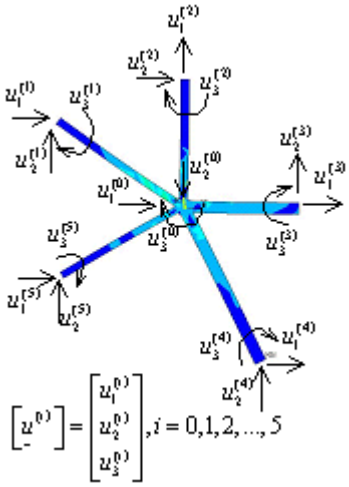

Figure 4. Stress plot for a Unit Truss

As shown in the stress plot of a sample unit lattice in Figure 5, the strain and stress around the nodes are usually complicated due to considerable inter-strut interactions and large bending moments. $\underset{\sim}{u}^{(i)}$ is the displacement of the node of the i^{th} strut in R^3. These results call into question the assumption regarding the pin-jointed behavior of vertices in other models.

An analytical model of unit lattices will be derived using continuum mechanics theory for both linear and non-linear elastic deformations. We assume that lattice struts behave like simple beams. The constitutive equation for a single strut is shown as Equation 1. Every strut has one equation and a unit lattice with N struts totally has N equations. $\underset{\sim}{\overline{K}}^{(i)}$ $(i=1,...,N)$ is the stiffness matrix of the i^{th} strut of a unit lattice in the local coordinate system. $\underset{\sim}{\overline{u}}^{(i)}$ and $\underset{\sim}{\overline{f}}^{(i)}$ represent displacements and forces respectively at the central node of the unit lattice for i = 0, and at nodes opposite to the central node for i = 1,2,…,N. Each node of the unit lattice has three degrees of freedom, among which two are primary variables (translational freedom, $u_1^{(i)}$ and $u_2^{(i)}$), and one is secondary variable (rotational freedom, $u_3^{(i)}$). Totally there are six degrees of freedom in this bending beam and the stiffness tensor of i^{th} strut of a horizontal unit lattice is 6×6 matrix shown as Equation 2 (Reddy, 1993).

$$\begin{bmatrix} \underset{\sim}{\overline{f}}^{(0)} \\ \cdots\cdots \\ \underset{\sim}{\overline{f}}^{(i)} \end{bmatrix} = \left[\underset{\sim}{\overline{K}}^{(i)}\right] \bullet \begin{bmatrix} \underset{\sim}{\overline{u}}^{(0)} \\ \cdots\cdots \\ \underset{\sim}{\overline{u}}^{(i)} \end{bmatrix}, \qquad i=1,2,...,N \qquad (1)$$

$$\left[\overline{\underset{\sim}{K}}^{(i)}\right] = \frac{2EI}{L^3}\left[\begin{array}{ccc:ccc} \mu & 0 & 0 & -\mu & 0 & 0 \\ 0 & 6 & -3L & 0 & -6 & -3L \\ 0 & -3L & 2L^2 & 0 & 3L & L^2 \\ \hdashline -\mu & 0 & 0 & \mu & 0 & 0 \\ 0 & -6 & 3L & 0 & 6 & 3L \\ 0 & -3L & L^2 & 0 & 3L & 2L^2 \end{array}\right]_{6\times 6} \qquad (2)$$

where: E = elastic modulus of solid material, I = moment of inertia of i^{th} strut, L = length of strut, A = area of strut cross-section, and $\mu = \frac{AL^2}{2I}$. The stiffness matrix must be rotated for non-horizontal struts using the standard rotation matrix, T, according to $\underset{\sim}{K}^{(i)} = \underset{\sim}{T}^T \bullet \overline{\underset{\sim}{K}}^{(i)} \bullet \underset{\sim}{T}$.

Therefore, the stiffness tensor of the m^{th} 2D unit lattice with N struts can be derived as:

$$\left[\underset{\sim}{\Psi}^{(m)}\right] = \left[\begin{array}{ccccc} \sum_{i=1}^{N}\Phi_{11}^{i} & \Phi_{12}^{1} & \Phi_{12}^{2} & \cdots & \Phi_{12}^{N} \\ \Phi_{21}^{1} & \Phi_{22}^{1} & 0 & \cdots & 0 \\ \Phi_{21}^{2} & 0 & \Phi_{22}^{2} & \cdots & 0 \\ \vdots & \vdots & \vdots & \ddots & \vdots \\ \Phi_{21}^{N} & 0 & 0 & \cdots & \Phi_{22}^{N} \end{array}\right]^{(m)}_{3(N+1)\times 3(N+1)} \qquad (3)$$

The components Φ_{11}^{i}, Φ_{12}^{i}, Φ_{21}^{i} and Φ_{22}^{i} (i = 0,1,…,N) are the 3×3 subsets of the 6×6 stiffness matrix $\left[\underset{\sim}{K}^{(i)}\right]$ of the i^{th} strut (Seepersad *et al*., 2004) shown as:

$$\left[\underset{\sim}{K}^{(i)}\right] = \left[\begin{array}{c:c} \Phi_{11}^{i} & \Phi_{12}^{i} \\ \hdashline \Phi_{21}^{i} & \Phi_{22}^{i} \end{array}\right]_{6\times 6} \qquad (4)$$

Therefore, the finite element model of this 2D unit lattice can be derived as:

$$\underset{\sim}{\Psi}^{(m)} \cdot \underset{\sim}{U}^{(m)} = \underset{\sim}{F}^{(m)} \qquad (5)$$

Similarly, the analytical model of 3D unit lattice in R^3 can be derived by a simple extension of the 2D model with the addition of torsion (Wang, 2005). In our model, we include beam bending, shearing, axial, and torsion effects. We also capture non-linearities arising from large deflections (geometric non-linearity) and material property behaviors (material non-linearity), as well as buckling failures. Each node in the 3D unit lattice has six degrees of freedom, so the stiffness matrix for a unit lattice with N struts will be $6N + 6$. The octet-truss unit cell (Fig. 1) will have 300 degrees of freedom.

The entire system can be analyzed in a quick and accurate manner through mathematically assembling the unit lattices, in a manner similar to that used in finite element analysis. The bilinear energy form of the whole structural system can be derived by assembling all unit lattices

together, as is shown in the following equation. *M* denotes the total number of unit latticees in the structural system (Bendsoe, 1995).

$$W_{in} = \sum_{m=1}^{M} W_{in}^{(m)}(\underset{\sim}{u}) = \sum_{m=1}^{M} \int_{\Omega^{(m)}} \frac{1}{2} \underset{\sim}{\varepsilon}(\underset{\sim}{u}) : \underset{\sim}{\tilde{E}}^{(m)} : \underset{\sim}{\varepsilon}(\underset{\sim}{u}) d\Omega^{(m)} \qquad (6)$$

The analytical modeling processes are similar for both design for rigidity and design for flexibility. To date, we have derived the analytical models of unit latticees in both 2D and 3D, and have implemented them (see Sec. 5). In 3D, the model contains tension/compression, bending, and torsion behaviors. Buckling considerations and nonlinear deformations have also been modeled (Wang, 2005).

3 MANUFACTURING METHODS FOR MESOSTRUCTURED MATERIALS

Various manufacturing methods have been developed for different types of mesostructure, but all have limitations in terms of macro- and meso-scale design freedom as well as material choice. For honeycombs, thin sheets of metal are stamped or crimped into a corrugated shape and then join to create ordered, hexagonal, cellular structures. Typically, thin strong skins are bonded to the lightweight honeycomb core to create sandwiches for heat resistant, low-density, structural applications (Cochran *et al*., 2000). Metal foams have specialized processes, each of which is limited typically to only one or a few types of metals (Ashby et al., 2000).

Uniform lattice structures were created by specialized casting techniques. Some groups use a combination of investment and vacuum casting (Chiras *et al*., 2002), while others have used sand casting. In both cases, a lattice structure pattern is fabricated using an additive manufacturing (AM) process, such as the SolidScape or ThermoJet (3D Systems) ink-jet printing machines, or the Fused Deposition Modeling technology from Stratasys.

Although these processes can cost-effectively create strong, lightweight, ordered cellular structures, their major limitation is a designer's inability to design either the macro- or mesostructure. For example, honeycombs are limited to only uniform, hexagonal, cellular structures. Not only do other cell shapes offer superior strength and stiffness, but it may be desirable to manufacture functionally graded cellular structures with variable cell sizes and topologies for specific applications. Foams are the result of a stochastic process. Casting has limitations on mesostructure size, complexity, and shape. Furthermore, there are difficulties with forming the cellular sandwiches into complex, non-planar shapes (Sypeck & Wadley, 2002).

The improvement of commercial AM technologies enabled production manufacturing applications of stereolithography (SL) and selective laser sintering (LS), in particular. For example, Siemens, Phonak, and Widex use SL and LS machines to produce hearing aid shells, Align Technology uses SL to fabricate molds for producing clear braces ("aligners"), and On-Demand Manufacturing uses LS to produce ducts and similar parts for F-18 fighter jets (Rosen *et al*., 2004). More generally, the unique capabilities of AM technologies enable new opportunities for customization, very significant improvements in product performance, multi-functionality, and lower overall manufacturing costs. Several research groups, including ours, have fabricated complex lattice structures using SL, LS, and other polymer-based processes.

However, it is the development of direct metal AM processes that ha expanded significantly the opportunities for designed mesostructure. Example processes include Arcam's electron beam melting (EBM) (Cormier *et al*., 2004), Laser Engineered Net Shaping (LENS), and MCP's Selective Laser Melting (Rosen *et al*., 2004), among others. Limitations still exist regarding feature size, shape complexity, and fabrication speed, but progress to date is promising.

4 SYNTHESIS METHODS FOR MESOSTRUCTURED MATERIALS

Synthesis methods are needed to determine the appropriate connectivity and sizes for lattice structures to achieve desired behaviors, including stiffness, strength, or deflected shapes. Minimum weight structures are typically desired as well. Two general synthesis methods are typical for shape and topology optimization, namely homogenization methods and ground truss approaches. Homogenization methods can be thought of as a point on-off ("material/no material") problem. They are often formulated using a material density function ρ where a point in a structure can be partially occupied by the structural material, with $\rho = 0$ corresponding to a void, $\rho = 1$ to solid material, and $0 < \rho < 1$ to the porous composite with voids at the micro level (Burns, 2002; Allaire & Kohn, 1993). In discrete ground truss approaches, the optimum topology is a subset of the ground truss, which is a complete graph of struts among all nodes. The cross-sections of the ground truss members are considered as continuous design variables for this optimization problem. The members with vanishing cross-sectional areas are removed to obtain the optimum (Burns, 2002). For a typical single load situation, the minimum compliance problem is formulated typically as minimizing compliance subject to static equilibrium and constant volume constraints (Bendsoe, 1995; Burns, 2002).

Our formulation of the lattice structure synthesis problem is based on the unit lattice, which replaces the microstructures in the homogenization method. The size of unit lattices is much larger than the porous rectangles of regular microstructures (Bendsoe, 1995), but much smaller than the lattice struts used in the ground truss approach (Allaire & Kohn, 1993).

The design of lightweight lattice structures is a problem of design for rigidity. Inefficient material will be removed for minimum material usage, but without compromising stiffness and strength. Our formulation of the lightweight truss structure problem is given in Figure 5, where the objective is to minimize the maximum nodal deflection subject to static equilibrium, axial stress, and material volume constraints. Diameters of lattice struts are the design variables represented by x_i and n is the number of struts in the initial topology of the structure. if we are more interested in minimizing the average nodal displacement, the total strain energy in the structure can replace the maximum nodal deflection objective. Only axial stress is considered since bending stresses are comparatively small.

Particle Swarm Optimization (PSO) and Generic Algorithms (GA) were selected from the available optimization algorithms to systematically search for design solutions. Compared to GA, PSO converges more quickly and was selected for the design synthesis of cellular structures (Fourie & Groenwold, 2002). PSO simulates the movement of birds in a flock (Kennedy & Eberhart, 1995), combining local search with global search. The authors developed the design synthesis method for lattice structures by integrating PSO with the unit lattice approach. Problems with hundreds of struts have been solved using this method.

Find:	$x = \{x_1, x_2, \cdots, x_n\}$	Diameters of lattice struts
Satisfy:	Bounds: $x_i \in \{0, [x_{min}, x_{max}]\}$	
	Constraints:	
	$h_1 : K \cdot U = F$	static equilibrium
	$g_1 : \sigma_{axial,i}(x) \leq \sigma_y$	axial stress
	$g_2 : V_{total} \leq V_{total,max}$	total material volume
Minimize:	$\max(U)$	maximum nodal deflection

Figure 5. Problem Formulation of Lightweight Truss Structure Design

For "design for flexibility" problems, the optimization model can be expressed in terms of maximum potential energy. In some cases, researchers formulated the problem in terms of the maximum ratio between mutual energy and strain energy (Frecker *et al*., 1997). The recent research on shape-morphing compliant mechanisms represents a good starting point for our work (Tai *et al*., 2002). Their single-input-multiple output mechanism problem formulations start with an initial lattice and enables mechanism connectivity information to be embedded in their design variables. Topology and shape optimization were performed simultaneously. Genetic algorithms were used to solve the problem. Methods for incorporating weight minimization, actuator forces, and other considerations were identified as issues for future work.

Research issues remain. For designed mesostructures, parts will consist of thousands to millions of lattice struts. The synthesis methods discussed here cannot handle such large problems. We will pursue approaches involving domain decomposition and multi-resolution models to address this. Most of the work in topology design and compliant mechanism synthesis has been limited to 2D problems; we require full 3D geometric complexity. The analysis models from Sec. 2 also have limitations. Homogenization approaches do not incorporate nonlinearities in material response. Ground truss approaches have not accounted for nonlinearities, even though compliant mechanisms are subject to large strains and often deform nonlinearly. Buckling is not considered in these models. Our analysis models incorporate material nonlinearities and will include buckling in the near future. We will utilize these analysis models in the proposed mesostructure synthesis research.

5 LATTICE STRUCTURE ANALYSIS

5.1 Multi-scale modeling of lattice structures

To analyze lattice structures, the geometric shape of the component is decomposed into mesostructure unit cells (structures possessing feature sizes between micro and macro-scales), as displayed in Fig. 6a, such that the mesostructures are used as the basic building blocks for the component geometry. Each mesostructure unit cell is further decomposed into smaller lattice structures (Fig. 6c) where the octet-truss structure (Fig. 6b) has been chosen to be the building blocks for each unit cell. Performing this decomposition creates a transition from the macro scale (component level) to the meso-scale (unit cell) and finally to the micro-scale (octet-truss).

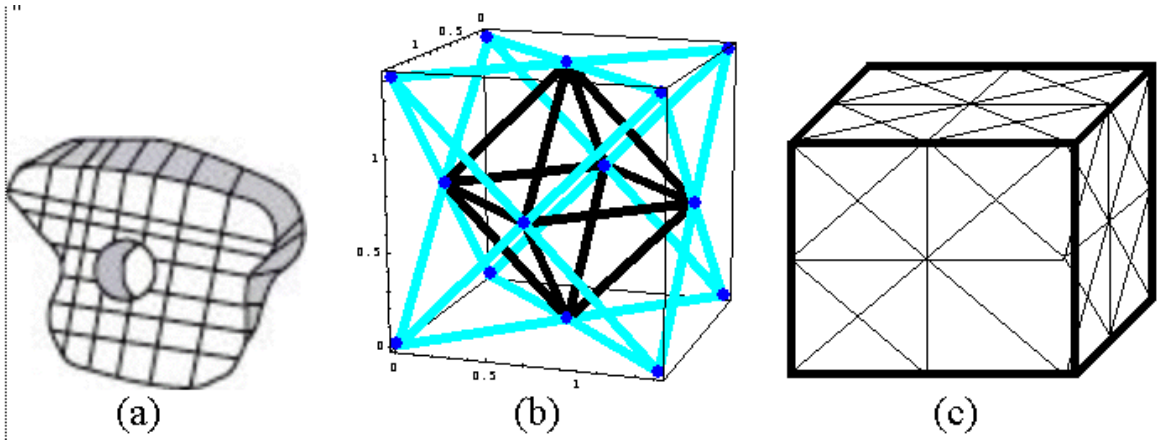

Figure 6. (a) Component geometry decomposed into unit cells, (b) octet-truss structure, and (c) a unit cell containing a 2 x 2 x 2 octet-truss structure.

The relative density of a unit cell will be used as a metric for characterization of the mechanical behavioral properties of the cell. The unit cell's relative density is determined by the thickness of each octet-truss strut and number of octet-truss structures located within the cell defined by

$$\bar{\rho} = 6\pi\sqrt{2}\left(\frac{a}{l}\right)^2 \qquad (7)$$

where a is the strut diameter and l is the length of each strut. Equation 7 represents the material volume of the inscribed unit cell containing an octet-truss structure, specifically, only half of the volume of each strut on each of the 6 faces is included because the remaining volume lies in the volume for adjacent cells. Each unit cell is analyzed for its stiffness and compliance with respect to the relative density to create a library of unit cells with known mechanical behavior. Unit cells containing n x n x n arrays of octet-truss structures are also be analyzed.

Unit cells comprised of octet truss structures are analyzed using a unit lattice finite element analysis (FEA) program in MATLAB that is an implementation of the 3D analysis model from Section 2 (Wang, 2005). The FEA program includes axial, bending, shearing, and torsion effects that are present in loading of the octet truss structure where previous analyses only included axial effects (Deshpande *et al*., 2001). The effective mechanical behavior of the unit cells using the unit truss FEA program will be discussed. Deshpande *et al*. (2001) have determined that the octahedral section of the octet-truss structure (central black structure in Fig. 6b) dominates the stiffness for the entire truss structure. However, they assume that the joints are pinned and only axial forces are present within the struts. The nodes of this central octahedral section are called the ***center nodes*** in this analysis, while the other nodes are called the ***corner nodes***.

The analysis of unit cells comprised of octet-truss structures is based on the approach used by Deshpande *et al*. by relating the relative stiffness (E/E_s) to the relative density ($\bar{\rho}$) for a fixed sized unit cell, where E_s is the elastic modulus for the solid strut material. The relative density is altered by varying the diameter of the struts of the octet-truss structure such that all of the struts will possess the same diameter within each unit cell.

According to our analysis, the relative stiffness values for a corner node and center node shown in Fig. 7a are almost identical in their mechanical behavior when the structure is assumed to be pinned. In contrast, Fig. 7b displays the effective stiffness for a single octet-truss structure under the same compressive load when the pin-jointed assumption is relaxed and bending, axial, and torsion effects are considered. Note that there is a significant difference in the relative stiffness of a corner node verses the center node. The stiffness at the center nodes is once again supported by the octahedral section of the octet-truss structure where the addition of the bending, shearing, and torsion effects have very little effect on the stiffness. The relative stiffness at a corner node is significantly reduced when these effects are included in the analysis as displayed by the bottom line in Fig. 7b.

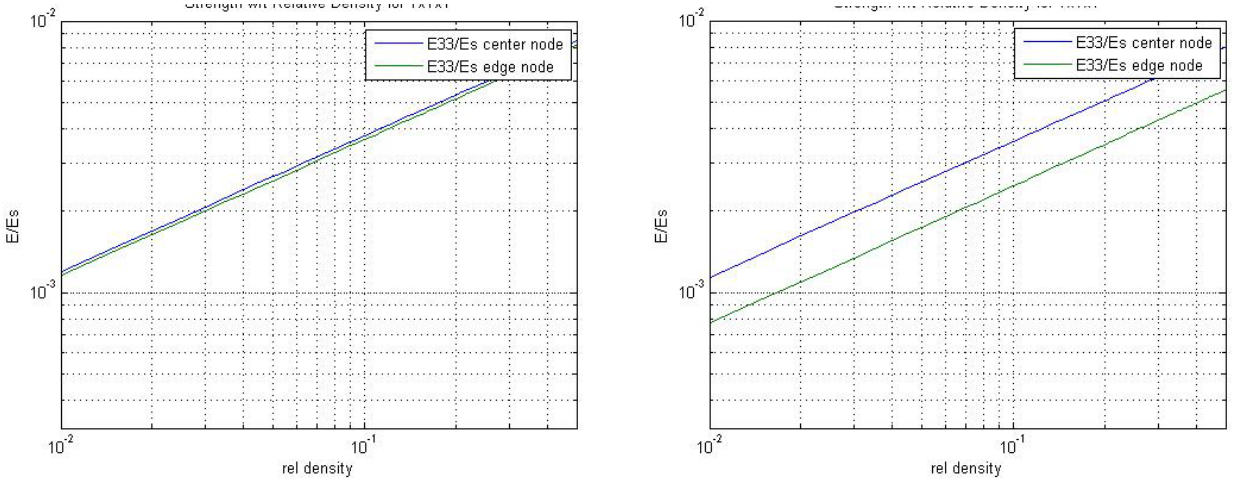

(a) (b)

Figure 7. Relative stiffness (E/E_s) for a single octet-truss structure under a uniform compressive load with respect to the relative density ($\bar{\rho}$), (a) for pinned joints which only include axial effects and (b) fully constrained joints.

Fig. 8 displays the same analysis results for a structure comprised of 3x3x3 octet-truss structures. A general trend of an increase in relative stiffness with respect to an increase in relative density is observed for both the pinned and fully constrained joints (portion a and b of each figure respectively). It can also be observed that the relative stiffness at interior nodes on the unit cell's exterior surface (top line) possess higher values than nodes on the edges of the unit cell (bottom line). The reason for this difference in relative stiffness is attributed to the presence of the supporting octahedral section of the octet-truss structures within the array of octets. The nodes at the edges must rely only on their connection to the octahedral sections for their stiffness.

A comparison between the relative stiffness of unit cells comprised of different size arrays of octets is enlightening. The relative stiffness of the unit cells decreases as the number of octet-truss structures increases. Specifically, a unit cell containing 27 (3x3x3) octet-truss structures (Fig. 10) has a lower relative stiffness at a fixed relative density compared to the single unit cell (and a 2x2x2 octet-truss structures, although not reported here). The dominant reason for this effect is caused by fixing the relative density of the unit cell, as this implies that strut diameters must decrease in size, which results in a more compliant unit cell.

The analysis of the octet-truss structure is the beginning of the next few steps for the mesostructure design synthesis. A library of the unit cells will be created after determining the behavior of various n x n x n arrays of octets under different loading conditions (non-uniform loads, shearing loads, and torsion).

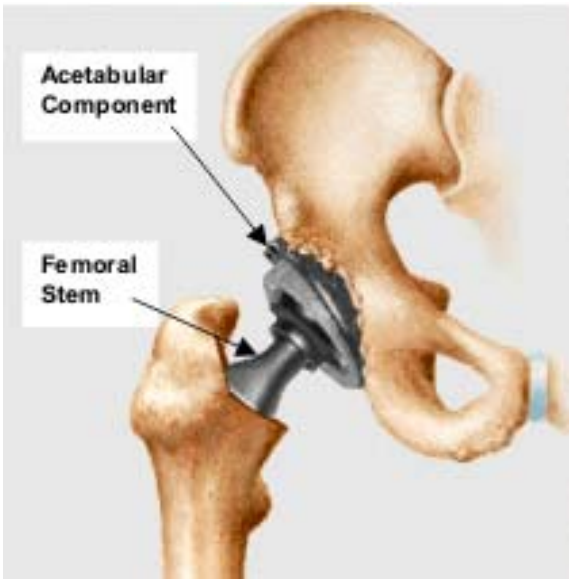

Figure 9. Hip joint replacement.

5.2 Hip joint example

We designed a component for a replacement hip joint that takes advantage of lattice structure to fulfill its two primary functions. A typical hip joint is shown in Fig. 10 (Medical, 2005). The acetabular component serves as the socket half of the ball-and-socket hip joint. Conventional acetabular components have a polyethylene liner to absorb impacts. In our design, impact absorption will be accommodated by designing a lattice structure implant that matches the stiffness of bone along the implant's outer region. During normal usage, the polyethylene liner is prone to wear, causing particles to break off, which can cause osteolysis, literally an "eating away" of the bone surrounding the implant. This causes aseptic mechanical loosening of the joint at the implant-bone interface, which is the major reason that the prostheses eventually fail (Chambers *et al*., 2004; Fitzgerald, 1992). The second function is to aid the fixation of the implant to the bone. The lattice structure's porosity will be designed to facilitate bone in-growth.

The natural porosity of the lattice structure can be used to enhance stability of the implant-bone interface. A new acetabular implant with gradient porosity will be developed for hip replacement. Porous coatings are popularly used in uncemented prostheses to make bone grow into implants for biological fixation (Bragdon *et al*., 2004). Gradient porous acetabular component with cellular structure will match the bone's elasticity. The interior region of the ilium around the acetabular component is spongy bone with average elasticity of 1GPa and yield strength of 5MPa. The exterior region of the ilium is compact bone with average elasticity of 16GPa and yield strength of 175MPa. The elasticity of the implanted acetabular component is desired to change gradually from 1GPa at its boundary to match the elasticity of the ilium. The geometric, stiffness, and porosity requirements are listed here:

- Shapes and sizes: hemispherical, with inner radius = 13.89mm and outer radius = 29.50mm
- Porosity (≥ 40% on implant-bone interface; solid on joint articulating interface)
- Pore size (≥ 0.2 mm; avoid space collapse and best interconnectivity)
- Effective elasticity: 1 GPa along outer lattice structure, grading to 16 GPa at edges, and to >90 GPa at interface to the solid socket.
- Adequate strength (≥ 500 MPa on articulating surface)

The final design is shown in Figure 13. A solid hemispherical shell is used for the socket. Lattice structure is used to provide porosity and to provide appropriate gradations in effective elasticity. Porosity of 91 percent is achieved at the outer surface using struts of 100 mm diameter and lengths of about 800-900 mm. The material selected is a titanium allow, Ti-6Al-4V, with an elastic modulus of 110 GPa. With the lattice struts of the chosen dimensions, the effective elasticity at the boundary is 1 GPa, achieving the desired elasticity. A tantalum carbide coating is used on the articulating surface to provide better wear resistance than the titanium alloy would provide.

6 CLOSURE

Our research project on the modeling, design, and manufacture of lattice-based cellular structures has been presented. We presented a new analytical model for lattice structure unit cells and outlined how models of large arrays of unit cells can be assembled in an FEA-like approach. Shape and topology synthesis methods were surveyed briefly and our formulation for rigid structure design was presented. Alternative manufacturing processes were investigated for their future applicability to lattice structure fabrication. We presented results showing that the stiffness of octet-truss structure decreases as the number of cells increase, for a fixed material density. These results are consistent with others reported in the literature; however, our model demonstrates that these structures are less stiff than would be predicted using simple truss models. In our hip joint example, we demonstrated the application of designed lattice structure for tailoring elasticity and porosity.

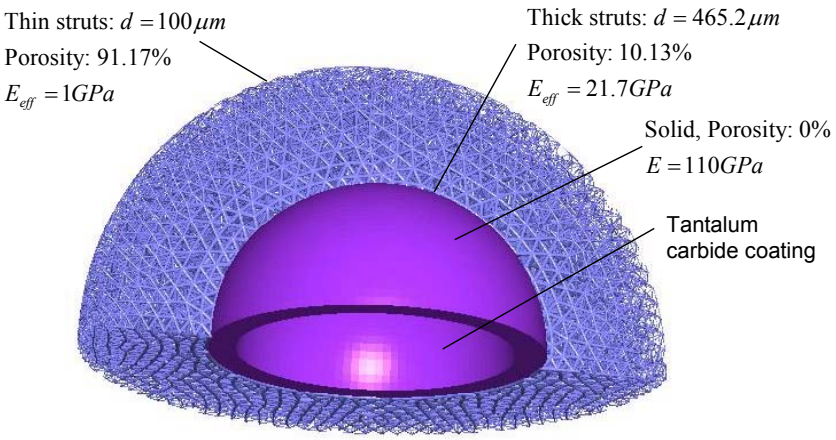

Figure 10. Lattice structure acetabular component.

7 ACKNOWLEDGEMENTS

We gratefully acknowledge the support of NSF through grant DMI-0522382.

8 REFERENCES

Allaire, G. and Kohn, R.V. (1993) Optimal design for minimum weight and compliance in plane stress using extremal microstructures. Europ. J. Mech. A/Solids, 12, 6, pp.839-878.
Ashby, M.F., Evans, A., Fleck, N. A., Gibson, L. J., Hutchinson, J. W., and Wadley, H. N. G. (2000) Metal Foams: A Design Guide. Woburn, MA: Butterworth-Heinemann.
Bendsoe, M.P. (1995) Optimization of structural topology, shape, and material, Springer-Verlag, Berlin Heidelberg.

Bendsoe, M.P., Kikuchi, N. (1988) Generating optimal Topologies in Structural Design using a Homogenization Method. Computer Methods in Applied Mechanics and Engineering, 71: 197-224, 1988.
Bragdon, C. R., Jasty, M. (2004) Biologic Fixation of Total Hip Implants. Journal of Bone & Joint Surgery **86** (Dec2004 Supplement): 105-117.
Burns, S.A. (2002) Recent advances in optimal structural design: American Society of Civil Engineers.
Chambers, I., K. F. Orishimo, et al., (2004) Relationship Between Polyethylene Wear and Osteolysis in Hips with a Second-Generation Porous-Coated Cementless Cup. Journal of Bone & Joint Surgery **86**(5): 1097 - 1098.
Chiras, S., Mumm, D.R., Evans, A.G., Wicks, N., Hutchinson, J.W., Dharmasena, K., Wadley, H.N.G., Fichter, S. (2002) The Structural Performance of Near-Optimized Truss Core Panels. Int'l, J. of Solids and Structures, 39(15):4093-4115.
Cochran, J. K., Lee, K. J., McDowell, D. L., and Sanders, T. H. (2000) Low Density Monolithic Honeycombs by Thermal Chemical Processing. Proceedings 4th Conference on Aerospace Materials, Processes, and Environmental Technology, Huntsville, AL.
Cormier, D., Harrysson, O., and West, H. (2004) Characterization of H13 Steel Produced via Electron Beam Melting. Rapid Prototyping Journal, 10(1):35-41.
Deshpande, V.S., Fleck, N.A., Ashby, M.F. (2001) Effective Properties of the Octet-Truss Lattice Material. J. of the Mechanics and Physics of Solids, Vol. 49, pp. 1747-1769.
Evans, A.G., Hutchinson, J.W., Fleck, N.A., Ashby, M.F., Wadley, H.N.G. (2001) The Topological Design of Multifunctional Cellular Materials. Progress in Materials Science, **46**(3-4):309-327, 2001.
Fitzgerald, R.H. (1992) Total hip arthroplasty sepsis. Orthopedic Clinics of North America **23**: 259-264.
Fourie, P.C., Groenwold, A.A., (2002) The particle swarm optimization algorithm in size and shape optimization. Structural and Multidisciplinary Optimization, vol. 23, pp. 259 - 267.
Frecker M.I., Ananthasuresh G.K., Nishiwaka S., Kikuchi, N., Kota S., (1997) Topological Synthesis of Compliant Mechanisms Using Multi-Criteria Optimization. ASME Transactions, Journal of Mechanical Design, Vol. 119, No. 2, pp. 238 -245.
Gibson, L. J., Ashby, M. F. (1997) Cellular Solids: Structure and Properties, Cambridge University Press, Cambridge, UK.
Jane's Information Group (2005) AAI RQ-7 Shadow 200. http://juav.janes.com/, September 13.
Kennedy, J., Eberhart, R.C. (1995) Particle Swam Optimization. Proc. IEEE International Conference on Neural Networks (Path, Australia), pp. 1942-1948.
Medical Multimedia Group (2005) A Patient's Guide to Total Hip Replacement Surgery. http://www.healthpages.org/AHP/ LIBRARY/HLTHTOP/THR/INDEX.HTM.
Reddy, J.N. (1993) An Introduction to the Finite Element Method. McGraw-Hill, Inc., New York.
Rosen, D.W., Atwood, C., Beaman, J., Bourell, D., Bergman, T., Hollister, S. (2004) Results of WTEC Additive/Substractive Manufacturing Study of European Research. Proc. SME Rapid Prototyping & Manufacturing Conference, paper # TP04PUB211, Dearborn, MI, May 10-13. Also, see: http://wtec.org/additive/welcome.htm for the complete report.
Seepersad, C.C., Dempsey, B.M., Allen, J.K., Mistree, F., McDowell, D.L. (2004) Design of Multifunctional Honeycomb Materials. AIAA Journal, Vol. 42, No. 5, pp.1025-1033.

Sypeck, D.J., Wadley, H.N.G. (2002) Cellular Metal Truss Core Sandwich Structures. Advanced Engineering Materials, **4**(10):759-764.
Tai, K., Cui, G.Y., Tapabrata, R. (2002) Design Synthesis of Path Generating Compliant Mechanisms by Evolutionary Optimization of Topology and Shape. ASME J. of Mechanical Design, 124, pp. 492-500.
Wang, A-J. and McDowell, D.L. (2005) Yield surfaces of various periodic metal honeycombs at intermediate relative density. International Journal of Plasticity, Volume 21, Issue 2, February pp. 285-320.
Wang, H. (2005) A Unit Cell Approach for Lightweight Cellular Structure and Compliant Mechanism. Ph.D. dissertation, Georgia Institute of Technology, 2005.
Wang, H., Rosen, D.W. (2002) Parametric Modeling Method for Truss Structures. ASME Computers and Information in Engineering Conference, DETC2002/CIE-34495, Montreal, Sept. 29-Oct 2.

